Electron-impact excitation of Co^{2+}

J. A. Shaw and M. S. Pindzola
Department of Physics, Auburn University, Auburn, Alabama 36849

N. R. Badnell
Department of Physics and Applied Physics, University of Strathclyde, Glasgow G4 0NG, United Kingdom

D. C. Griffin
Department of Physics, Rollins College, Winter Park, Florida 32789

(Received 1 April 1998)

Electron-impact excitation cross sections and Maxwellian-averaged rate coefficients are calculated from the ground $3d^7\ ^4F$ to the first $3d^7\ ^4P$ and the second $3d^7\ ^2G$ excited terms in Co^{2+} in close coupling with 8 and 27 terms; much larger transition arrays were first explored in a distorted-wave approximation. Both transitions are important elements of the emission spectrum of type Ia supernovae. We find that the two excitations are dominated by autoionizing resonances attached to higher-lying excited terms in the $3d^7$, $3d^6 4s$, $3d^6 4p$, and $3d^6 4d$ configurations. Those LS terms that are strongly excited from the ground $3d^7\ ^4F$, as found by distorted-wave calculations, are included in a large R-matrix calculation using asymptotics based on multichannel quantum defect theory. [S1050-2947(98)06510-X]

PACS number(s): 34.80.Kw

I. INTRODUCTION

The electron-impact excitation and radiative rates of Co^+ and Co^{2+} in low-temperature plasmas are needed to calculate the populations of these ions for the observed spectra of astrophysical plasmas. The evolution of the spectrum of type Ia supernovae with time shows features that can be attributed to the low ionization stages of cobalt [1]. Atomic structure calculations are generally difficult for these ions because of the many LS terms arising from open d-shell configurations. The terms of the two lowest-energy configurations for Co^+ are interleaved, i.e., terms from one configuration alternate with the terms from the other configuration, so even getting the order of these energy levels would require an elaborate configuration-interaction calculation involving hundreds of terms. The terms of the two lowest-energy configurations of Co^{2+} are, in contrast, almost completely separated [2,3], so it is relatively easy to get the order of the lowest-energy levels and their spacing to moderate accuracy with a much smaller calculation. However, accurate calculations of the energy levels are still difficult.

In this paper we carry out a series of distorted-wave and close-coupling calculations for the electron-impact excitation cross sections and rate coefficients of the two lowest-energy transitions in Co^{2+}. The ground configuration of Co^{2+} is $3d^7$ and contains, from lowest to highest energy, eight terms ^4F, ^4P, ^2G, ^2P, ^2D, ^2H, ^2F, and ^2D. The main radiative lines seen in the supernova spectrum arise from the forbidden transitions $3d^7\ ^4P \rightarrow 3d^7\ ^4F$ and $3d^7\ ^2G \rightarrow 3d^7\ ^4F$ [1]. The excited $3d^6 4\ell$ ($\ell = 0,1,2,3$) configurations contain an additional 324 LS terms, but the lowest LS terms begin 7.0 eV above the ground $3d^7\ ^4F$ and are thus not important at the low thermal electron temperatures (0.1–2.0 eV) characteristic of type Ia supernovae. However, the autoionizing resonances attached to these excited configurations can significantly enhance the $3d^7\ ^4F \rightarrow 3d^7\ ^4P$ and $3d^7\ ^4F \rightarrow 3d^7\ ^2G$ excitations. In previous work [4,5] on the isoelectronic Fe^+ atomic ion, resonances attached to the $3d^6 4p$ configuration were found to make strong contributions to the excitation cross sections among the LS terms of the $3d^7$ and $3d^6 4s$ configurations. In the present work, we find that resonances attached to the $3d^6 4\ell$ ($\ell = 0,1,2$) configurations all make strong contributions to the excitation cross sections among the LS terms of the $3d^7$ configuration of Co^{2+}. We note also related work on Ni^+ [6] and Ni^{2+} [7], which makes use of the RMATRX II code [8].

The remainder of this paper is organized in the following manner. In Sec. II we carry out a series of configuration-average and LS term explicit distorted-wave calculations to determine the strongest excitations from the ground $3d^7\ ^4F$ of Co^{2+}. In Sec. III we carry out a series of R-matrix close-coupling calculations involving excitation strength ordered

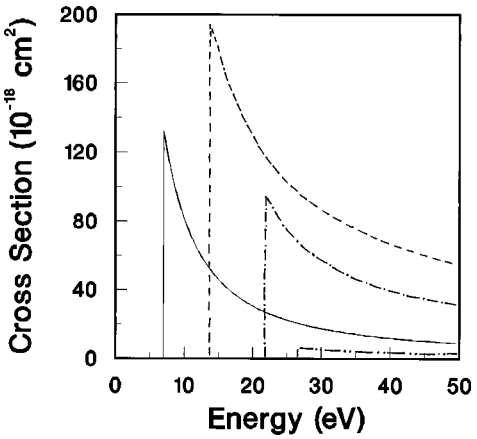

FIG. 1. Configuration-average distorted-wave cross sections for Co^{2+}. Solid line: $3d^7 \rightarrow 3d^6 4s$ excitation, dashed line: $3d^7 \rightarrow 3d^6 4p$ excitation, dashed-dotted line: $3d^7 \rightarrow 3d^6 4d$ excitation, and dashed–double-dotted line: $3d^7 \rightarrow 3d^6 4f$ excitation.

TABLE I. Distorted-wave cross sections for the $3d^7\ ^4F \rightarrow 3d^7\ ^{2S+1}L$ and $3d^7\ ^4F \rightarrow 3d^6 4\ell$ ($\ell = 0,1,2$)^{2S+1}L excitations in Co^{2+}. There are a total of 203 excitations, of which we list the 54 cross sections with magnitudes greater than 1.0×10^{-18} cm^2.

Index	Configuration	Term	Threshold energy (eV)	Threshold cross section (10^{-18} cm^2)	Index	Configuration	Term	Threshold energy (eV)	Threshold cross section (10^{-18} cm^2)
1	$3d^7$	^4P	2.07	198.30	10	$3d^6\ 4p$	$^2G^o$	17.45	1.33
2	$3d^7$	^2G	2.35	233.01	11	$3d^6\ 4p$	$^4F^o$	17.51	2.37
3	$3d^7$	^2P	2.81	49.49	12	$3d^6\ 4p$	$^2I^o$	17.56	1.86
4	$3d^7$	^2D	3.02	79.98	13	$3d^6\ 4p$	$^4D^o$	17.71	1.30
5	$3d^7$	^2H	3.27	164.77	14	$3d^6\ 4p$	$^4D^o$	17.85	13.65
6	$3d^7$	^2F	5.23	35.63	15	$3d^6\ 4p$	$^4G^o$	17.92	10.41
7	$3d^7$	^2D	7.82	12.99	16	$3d^6\ 4p$	$^4G^o$	17.99	3.78
1	$3d^6\ 4s$	^6D	7.44	14.48	17	$3d^6\ 4p$	$^2H^o$	18.03	1.10
2	$3d^6\ 4s$	^4D	9.08	16.62	18	$3d^6\ 4p$	$^4H^o$	18.11	2.29
3	$3d^6\ 4s$	^4H	10.69	10.53	19	$3d^6\ 4p$	$^4F^o$	18.17	16.37
4	$3d^6\ 4s$	^4P	11.03	2.74	1	$3d^6\ 4d$	^6F	22.15	3.05
5	$3d^6\ 4s$	^4F	11.13	4.15	2	$3d^6\ 4d$	^6D	22.36	2.15
6	$3d^6\ 4s$	^4G	11.46	7.85	3	$3d^6\ 4d$	^6P	22.47	1.12
7	$3d^6\ 4s$	^2H	11.67	2.69	4	$3d^6\ 4d$	^6G	22.50	3.57
8	$3d^6\ 4s$	^2F	12.11	1.05	5	$3d^6\ 4d$	^4D	22.73	1.69
9	$3d^6\ 4s$	^2G	12.44	2.00	6	$3d^6\ 4d$	^4G	22.81	2.83
10	$3d^6\ 4s$	^4D	12.54	1.18	7	$3d^6\ 4d$	^4F	23.11	8.27
11	$3d^6\ 4s$	^4F	15.68	1.43	8	$3d^6\ 4d$	^4J	25.32	1.71
1	$3d^6\ 4p$	$^6D^o$	13.59	7.04	9	$3d^6\ 4d$	^4H	25.36	1.08
2	$3d^6\ 4p$	$^6F^o$	14.28	7.56	10	$3d^6\ 4d$	^4I	25.39	1.27
3	$3d^6\ 4p$	$^6P^o$	14.66	2.74	11	$3d^6\ 4d$	^4F	26.06	1.17
4	$3d^6\ 4p$	$^4D^o$	15.08	22.41	12	$3d^6\ 4d$	^4H	26.16	1.22
5	$3d^6\ 4p$	$^4F^o$	15.11	13.81	13	$3d^6\ 4d$	^4I	26.20	1.21
6	$3d^6\ 4p$	$^4P^o$	15.62	1.58	14	$3d^6\ 4d$	^4F	27.24	1.05
7	$3d^6\ 4p$	$^4G^o$	17.14	13.90	15	$3d^6\ 4d$	^4F	28.73	29.93
8	$3d^6\ 4p$	$^4I^o$	17.16	3.64	16	$3d^6\ 4d$	^4F	30.37	1.46
9	$3d^6\ 4p$	$^4H^o$	17.18	2.55	17	$3d^6\ 4d$	^4F	31.13	5.23

subsets of the 204 LS terms available in the $3d^7$ and $3d^6 4\ell$ ($\ell = 0,1,2$) configurations of Co^{2+}. Extensive use is made of the pseudoresonance removal procedure developed by Gorczyca *et al.* [9], since only selected terms from each configuration are included in the close-coupling expansion. We employ an asymptotic coupled equations method based on multichannel quantum defect theory [10,11] to map out resonance structures in the threshold region for the $3d^7\ ^4F \rightarrow 3d^7\ ^4P$ and $3d^7\ ^4F \rightarrow 3d^7\ ^2G$ excitations. The cross sections are then integrated over a Maxwellian energy distribution to yield rate coefficients. We conclude in Sec. IV with a brief summary of the present work.

II. DISTORTED-WAVE CALCULATIONS

The guiding principle in this section is that a series of distorted-wave excitation calculations may help us choose the LS terms needed to make an accurate R-matrix calculation for the $3d^7\ ^4F \rightarrow 3d^7\ ^4P$ and ^2G transitions in Co^{2+}. The LS terms associated with the $3d^6 4\ell$ ($\ell = 0,1,2,3$) configurations may have a strong affect on the low-lying excitations of interest through the autoionizing resonances attached to them. In such a complex ion as Co^{2+} we cannot yet include all the 324 LS terms in a brute force manner. By examining the distorted-wave calculations we hope to identify those LS terms in the $3d^6\ 4\ell$ ($\ell = 0,1,2,3$) configurations which are strongly coupled to the $3d^7\ ^4F$ ground LS term.

We begin with distorted-wave calculations for excitations between the ground and first four excited configurations of Co^{2+}. In Fig. 1 we present cross sections for the $3d^7 \rightarrow 3d^6 4\ell$ ($\ell = 0,1,2,3$) excitations calculated in a configuration-average distorted-wave approximation [12]. The bound-state orbitals are calculated in a configuration-average Hartree-Fock approximation using Cowan's atomic wave-function code [13]. Since the radial orbitals do not vary over a configuration, an algebraic average over all states of an initial configuration and an algebraic sum over all states of a final configuration reduces the cross-section expression to a quite simple form. Thus, for example, a configuration-average distorted-wave cross section involving the 8 LS terms of the $3d^7$ initial configuration and the 128 LS terms of the $3d^6 4f$ final configuration can be calculated quite quickly in practice. From Fig. 1, we see that excitations to the $3d^6 4\ell$ ($\ell = 0,1,2$) configurations are much larger than the excitation to the $3d^6 4f$ configuration. Thus, we drop the many LS terms associated with the $3d^6 4f$ configuration as possible ''sources'' of resonances that may strongly affect the $3d^7\ ^4F \rightarrow 3d^7\ ^4P$ and ^2G excitation cross sections of interest in Co^{2+}.

TABLE II. Eigenenergies and configuration-term label of the eigenstates for the eight-term R-matrix calculation. There are a total of 44 eigenstates from the atomic structure calculation.

Index	Configuration	Term	Theoretical energy (eV)	Experimental energy [2] (eV)
1	$3d^7$	^4F	0.00	0.00
2	$3d^7$	^4P	2.12	1.91
3	$3d^7$	^2G	2.32	2.15
4	$3d^7$	^2P	2.79	2.53
5	$3d^7$	^2D	3.00	2.92
6	$3d^7$	^2H	3.26	2.86
7	$3d^7$	^2F	5.26	4.61
8	$3d^7$	^2D	7.87	6.98

We next carried out distorted-wave calculations for excitations between the $3d^7\ ^4F$ ground LS term and the remaining LS terms in the $3d^7$ configuration and all the LS terms in the $3d^6 4\ell$ ($\ell=0,1,2$) configurations of Co^{2+}. In Table I we present all of the $3d^7\ ^4F \rightarrow 3d^7, 3d^6 4\ell$ ($\ell=0,1,2$) ^{2S+1}L excitations calculated in a configuration-interaction LS distorted-wave approximation that have cross sections with magnitudes greater than 1.00 Mb (1.0 Mb$=1.0\times10^{-18}$ cm^2). The bound-state orbitals are calculated in a configuration-average Hartree-Fock approximation using Froese Fischer's atomic wave function code [14]. The distorted-wave cross sections are calculated using an extensively modified version of the Belfast atomic R-matrix codes [15]. Briefly, the STG1 and STG2 codes are used in LS mode to generate configuration-interaction N-electron bound-state wave functions and $(N+1)$-electron scattering algebra. A code named STGDW then calculates nonunitarized LS distorted-wave cross sections. From Table I, we see that the two largest excitations from the $3d^7\ ^4F$ ground term are to the $3d^7\ ^4P$ first excited and $3d^7\ ^2G$ second excited terms. All the LS terms in the ground configuration have relatively large excitation cross sections. The strongest excitation cross sections in the $3d^6 4s$ configuration belong to the ^6D, ^4D, and ^4H symmetries, the largest in the $3d^6 4p$ configuration belong to the $^4D^o$, $^4F^o$, and $^4G^o$ symmetries, while the largest in the $3d^6 4d$ configuration belong to the ^4F symmetry. Although in principle we also need an estimate of the coupling of the $3d^7\ ^4P$ and $3d^7\ ^2G$ terms to the higher LS terms in the $3d^6 4\ell$ ($\ell=0,1,2$) configurations, we will use just the distorted-wave calculations described above to help us choose the LS terms needed to make an accurate R-matrix calculation for Co^{2+}.

III. R-MATRIX CALCULATIONS

A. Close-coupling expansion involving eight LS terms

We first carried out an R-matrix calculation involving eight LS terms in the close-coupling expansion. An orthogonal set of bound-state orbitals are calculated in a configuration-average Hartree-Fock approximation using Froese Fischer's atomic wave-function code [14]. The R-matrix cross sections are calculated using an extensively modified version of the Belfast codes [15]. The N-electron bound-state wave functions included configuration-interaction among the 44 LS terms in the $3p^6 3d^7$, $3p^6 3d^6 4s$, and $3p^4 3d^9$ even-parity configurations. In previous work [16], the addition of the $3p^6 3d^5 4s^2$ configuration was shown to have little effect on the excitation energies. In Table II we list the eigenenergies and the configuration-term label of the eigenstates for the R-matrix calculation. Thus, the close-coupling expansion includes all eight LS terms of the $3d^7$ ground configuration. As seen in Table II, the overall agreement between theory and experiment for the energies of the eight LS terms is at the 10% level, with only the ^2D and ^2H terms switched in the relative ordering.

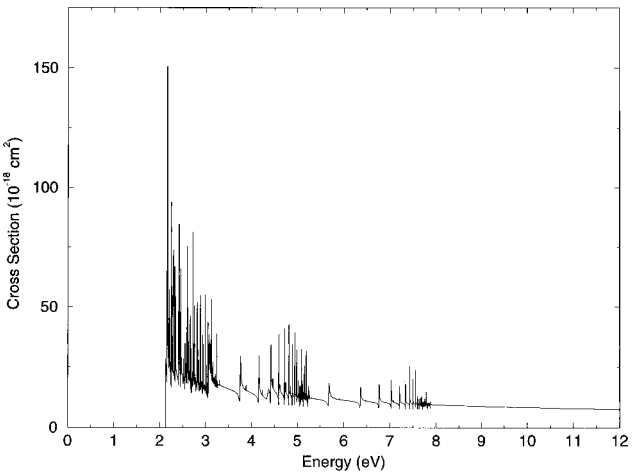

FIG. 2. Eight-term R-matrix cross section for the $3d^7\ ^4F \rightarrow 3d^7\ ^4P$ excitation in Co^{2+}.

The eight-term R-matrix cross sections for the $3d^7\ ^4F \rightarrow 3d^7\ ^4P$ and the $3d^7\ ^4F \rightarrow 3d^7\ ^2G$ transitions are presented in Figs. 2 and 3. Any nonphysical pseudoresonances associated with the eigenstates included in the N-electron bound-state wave function, but not included in the close-coupling expansion, are removed using the transformation matrix method of Gorczyca *et al.* [9]. The angular momentum of the $(N+1)$-electron system was taken up to $L=11$, enough to ensure the convergence of these quadrupole and spin forbidden transitions. The background excitation cross section at threshold for the $3d^7\ ^4F \rightarrow 3d^7\ ^4P$ quadrupole

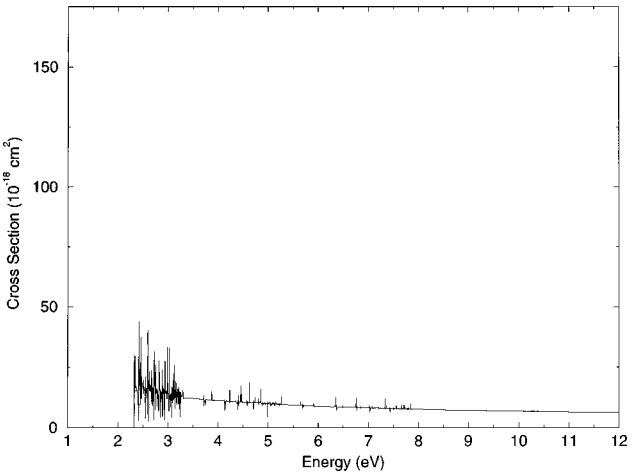

FIG. 3. Eight-term R-matrix cross section for the $3d^7\ ^4F \rightarrow 3d^7\ ^2G$ excitation in Co^{2+}.

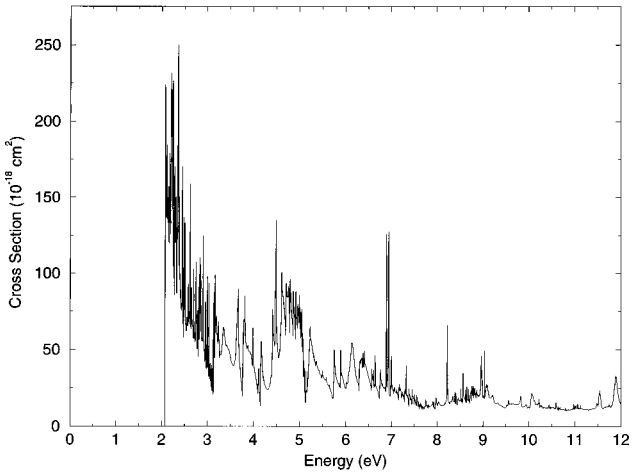

FIG. 4. Twenty-seven-term R-matrix cross section for the $3d^7\ ^4F \rightarrow 3d^7\ ^4P$ excitation in Co^{2+}.

transition is around 30 Mb, in sharp contrast to the 198 Mb predicted by distorted-wave theory in Table I. The background cross section at threshold for the $3d^7\ ^4F \rightarrow 3d^7\ ^2G$ spin-changing transition is around 20 Mb, more than an order of magnitude smaller than the distorted-wave prediction of 233 Mb. Obviously, there are strong coupling effects among the eight LS terms in the eigenfunction expansion. At this point, we repeated the distorted-wave calculations, including unitarization among the 8 LS terms of the $3d^7$ configuration, and found a substantial decrease in the cross-section predictions. This serves as a further indication of strong coupling effects. From Figs. 2 and 3, we see that both excitations are dominated by strong autoionizing resonances in the threshold region. Since the electron-impact excitation Maxwellian rate coefficients are needed at temperatures ranging from 0.1 to 2.0 eV, the near threshold resonances will play a major role in determining the size of those rates.

B. Close-coupling expansion involving 27 LS terms

We next carried out an R-matrix calculation involving 27 LS terms in the close-coupling expansion. The N-electron bound-state wave functions included configuration-interaction among the 148 LS terms in the $3p^6 3d^7$, $3p^6 3d^6 4s$, $3p^6 3d^6 4d$, and $3p^4 3d^9$ even-parity configurations and term mixing among the 68 LS terms in the $3p^6 3d^6 4p$ odd-parity configuration. In Table III we list the

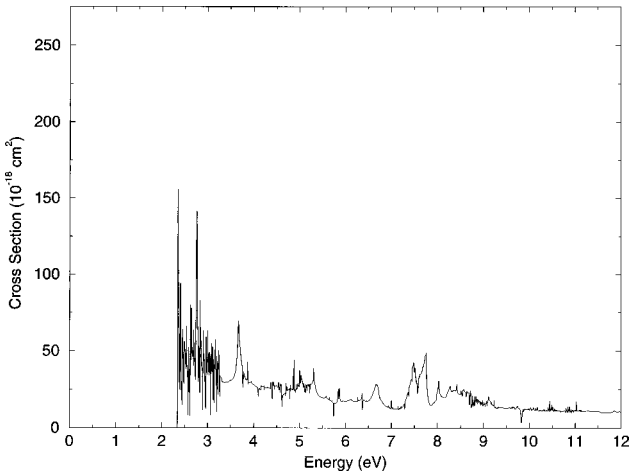

FIG. 5. Twenty-seven-term R-matrix cross section for the $3d^7\ ^4F \rightarrow 3d^7\ ^2G$ excitation in Co^{2+}.

TABLE III. Eigenenergies and configuration-term label of the eigenstates for the 27-term R-matrix calculation. There are a total of 216 eigenstates from the atomic structure calculation.

Index	Configuration	Term	Theoretical Energy	Experimental energy [2]
1	$3d^7$	^4F	0.00	0.00
2	$3d^7$	^4P	2.07	1.91
3	$3d^7$	^2G	2.35	2.15
4	$3d^7$	^2P	2.81	2.53
5	$3d^7$	^2D	3.01	2.92
6	$3d^7$	^2H	3.27	2.86
7	$3d^7$	^2F	5.23	4.61
8	$3d^6\ 4s$	^6D	7.44	
9	$3d^7$	^2D	7.82	6.98
10	$3d^6\ 4s$	^4D	9.08	
11	$3d^6\ 4s$	^4H	10.69	
12	$3d^6\ 4s$	^4F	11.13	
13	$3d^6\ 4p$	$^4D^o$	15.08	
14	$3d^6\ 4p$	$^4F^o$	15.11	
15	$3d^6\ 4s$	^4F	15.68	
16	$3d^6\ 4p$	$^4G^o$	17.14	
17	$3d^6\ 4p$	$^4F^o$	17.51	
18	$3d^6\ 4p$	$^4D^o$	17.71	
19	$3d^6\ 4p$	$^4D^o$	17.85	
20	$3d^6\ 4p$	$^4G^o$	17.92	
21	$3d^6\ 4p$	$^4F^o$	18.17	
22	$3d^6\ 4d$	^4F	23.11	
23	$3d^6\ 4d$	^4F	25.53	
24	$3d^6\ 4d$	^4F	25.87	
25	$3d^6\ 4d$	^4F	26.06	
26	$3d^6\ 4d$	^4F	27.24	
27	$3d^6\ 4d$	^4F	28.73	

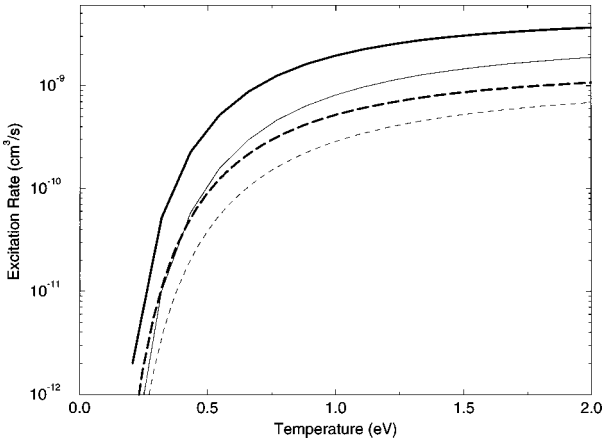

FIG. 6. Maxwellian-averaged excitation rate coefficients for Co^{2+} from R-matrix calculations. The transition $3d^7\ ^4F \rightarrow 3d^7\ ^4P$ is in heavy lines: solid for 27 terms, dashed for eight terms. The transition $3d^7\ ^4F \rightarrow 3d^7\ ^2G$ is in light lines: solid or dashed as above.

eigenenergies and the configuration-term label of the eigenstates for the R-matrix calculation. Guided by the LS distorted-wave calculations of Sec. II, we chose the 27 LS terms in the close-coupling expansion to include all eight LS terms of the $3d^7$ ground configuration, the 10 LS terms associated with the strongest $3d^7 \rightarrow 3d^6 4\ell$ ($\ell = 0,1,2$) excitations, and nine more LS terms of the same symmetry as the strongest 18.

The 27-term R-matrix cross sections for the $3d^7\ ^4F \rightarrow 3d^7\ ^4P$ and $3d^7\ ^4F \rightarrow 3d^7\ ^2G$ transitions are presented in Figs. 4 and 5. Any pseudoresonances that may be attached to eigenstates in the N-electron bound-state wave function, but not included in the close-coupling expansion, are removed using the transformation matrix method [9]. The computational time needed for the 27-term R-matrix calculations was considerably shortened through the use of a new version of the asymptotic coupled equations code named STGF [17,18]. Basically, unphysical K matrices are calculated on a coarse energy mesh and multichannel quantum defect theory (MQDT) is used to determine the physical K matrices, and thus the cross sections, on a fine energy mesh [11]. Interpolation of the unphysical K matrix and calculation of the MQDT transformation is much faster than direct calculation at each energy point. For a system like Co^{2+}, with many resonances in the threshold region, the new STGF calculations are an order of magnitude faster. Comparing Fig. 2 from the 8-term calculation and Fig. 4 from the 27-term calculation, we see that the excitation cross section at threshold for the $3d^7\ ^4F \rightarrow 3d^7\ ^4P$ quadrupole transition has been strongly enhanced by the additional resonance structures found in the larger R-matrix calculation. A comparison of Figs. 3 and 5 shows that the cross section for the $3d^7\ ^4F \rightarrow 3d^7\ ^2G$ spin-changing transition has also been strongly enhanced by additional autoionizing resonances.

C. Maxwellian-averaged excitation rates

Maxwellian-averaged excitation rate coefficients are calculated by integration over the R-matrix cross sections found in Figs. 2–5. A fine mesh spacing of 0.000 24 eV was used in the range 1.9–3.0 eV and a coarser mesh spacing of 0.0024 eV was used from 3.0 to 11.5 eV. At 11.5 eV the 8-term calculation was extended to higher energy by fitting to an analytic form above the highest thresholds. The 27-term calculation was continued on a coarse mesh spacing of 0.007 eV until 30 eV. This was sufficiently high in energy that the effect on the nondipole excitation rates in the range 0.1 to 2.0 eV was negligible. The R-matrix rate coefficients for the $3d^7\ ^4F \rightarrow 3d^7\ ^4P$ and $3d^7\ ^4F \rightarrow 3d^7\ ^2G$ transitions are presented in Fig. 6. The additional resonance structures found in the larger R-matrix calculation are found to strongly enhance both excitation rate coefficients in the temperature range from 0.1 to 2.0 eV.

IV. CONCLUSIONS

We have calculated LS resolved electron-impact cross sections for Co^{2+} and used these to obtain excitation rates needed for supernovae modeling. The open d-shell makes these calculations difficult. The atomic structure is hard to determine accurately and resonant enhancement of the cross sections is large. To address this problem we used distorted-wave calculations to find those LS terms that should have particularly strong resonance enhancements and included these in the close-coupling expansion while eliminating possible pseudoresonances. This general procedure can be applied to other atomic ions and should give improved estimates of cross sections and rate coefficients. The use of multichannel quantum-defect theory in the asymptotic code allowed for rapid calculation of the cross sections compared to the usual methods. A term coupling plus frame transformation calculation can be performed in the same manner and this may be done in the future. The excitation rate coefficients from this calculation will become part of the database at the Controlled Fusion Atomic Data Center at Oak Ridge National Laboratory.

ACKNOWLEDGMENTS

This work was supported in part by the U.S. Department of Energy under Grant No. DE-FG05-96-ER54348 with Auburn University, Grant No. DE-FG02-96-ER54367 with Rollins College, and by the EPSRC under Grant No. GR/K/14346 with the University of Strathclyde.

[1] W. Liu, D. Jeffery, D. R. Schultz, P. Quinet, J. A. Shaw, and M. S. Pindzola, Astrophys. J. Lett. **489**, L141 (1997).

[2] J. Sugar and C. Corliss, J. Phys. Chem. Ref. Data **10**, 1116 (1981).

[3] C. Moore, *Atomic Energy Levels: Vol. II*, NSRDS-MBS No. 35 (U.S. Government Printing Office, Washington, D.C., 1971).

[4] A. K. Pradhan and K. A. Berrington, J. Phys. B **26**, 157 (1993).

[5] H. L. Zhang and A. K. Pradhan, Astron. Astrophys. **293**, 953 (1995).

[6] M. S. T. Watts, K. A. Berrington, P. G. Burke, and V. M. Burke, J. Phys. B **29**, L505 (1996).

[7] M. S. T. Watts and V. M. Burke, J. Phys. B **31**, 145 (1998).

[8] P. G. Burke, V. M. Burke, and K. M. Dunseath, J. Phys. B **27**, 5341 (1994).

[9] T. W. Gorczyca, F. Robicheaux, M. S. Pindzola, D. C. Griffin, and N. R. Badnell, Phys. Rev. A **52**, 3877 (1995).

[10] M. Aymar, C. H. Greene, and E. Luc-Koenig, Rev. Mod. Phys. **68**, 1015 (1996).

[11] N. R. Badnell, T. W. Gorczyca, and A. D. Price, J. Phys. B **31**, L239 (1998).

[12] M. S. Pindzola, D. C. Griffin, and C. Bottcher, *Atomic Processes in Electron-Ion and Ion-Ion Collisions*, Vol. 145 of NATO Advanced Studies Institute Series B: Physics (Plenum, New York, 1986), p. 75.
[13] R. D. Cowan, *The Theory of Atomic Structure and Spectra* (University of California Press, Berkeley, 1981).
[14] C. Froese Fischer, Comput. Phys. Commun. **64**, 369 (1991).
[15] K. A. Berrington, W. B. Eissner, and P. H. Norrington, Comput. Phys. Commun. **92**, 290 (1995).
[16] Y. Shadmi, E. Caspi, and J. Oreg, J. Res. Natl. Bur. Stand-.Sect. A **73**, 173 (1969).
[17] M. J. Seaton, J. Phys. B **14**, 3827 (1981); **18**, 2111 (1985); **19**, 2601 (1986).
[18] K. A. Berrington, P. G. Burke, K. Butler, M. J. Seaton, P. J. Storey, K. T. Taylor, and Yu Yan, J. Phys. B **20**, 3827 (1987).